Kinetic and thermodynamic driving factors in the assembly of phenylalanine-based modules

Dor Zaguri[1,†], Manuela R. Zimmermann[2,†], Georg Meisl[2], Aviad Levin[2], Sigal Rencus-Lazar[1], Tuomas P. J. Knowles[2,3,*], and Ehud Gazit[1,4,*]

[1] The Shmunis School of Biomedicine and Cancer Research, Tel Aviv University, Tel Aviv 6997801, Israel.

[2] Yusuf Hamied Department of Chemistry, University of Cambridge, Cambridge, CB2 1EW, United Kingdom.

[3] Cavendish Laboratory, University of Cambridge, Cambridge, CB3 0HE, United Kingdom.

[4] BLAVATNIK CENTER for Drug Discovery for Drug Discovery, Tel Aviv University, Tel Aviv 6997801, Israel.

[†] These authors contributed equally: D. Zaguri and M.R. Zimmermann.
[*] To whom correspondence should be addressed: tpjk2@cam.ac.uk and ehudga@tauex.tau.ac.il.

Abstract

The formation of ordered protein and peptide assemblies is a phenomenon related to a wide range of human diseases. However, the mechanism of assembly at the molecular level remains largely unknown. Minimal models enable the exploration of the underlying interactions that are at the core of such self-assembly processes. In particular, the ability of phenylalanine, a single aromatic amino acid, to form amyloid-like structure, has challenged the previous dogma viewing a peptide backbone as a prerequisite for assembly. The driving forces controlling the nucleation and assembly in the absence of a peptide backbone remain to be identified. Here, aiming to unravel these forces, we explored the kinetics and thermodynamics of three phenylalanine-containing molecules during their assembly process: the amino acid phenylalanine, which accumulates in phenylketonuria patients, the diphenylalanine core-motif of the amyloid beta peptide related to Alzheimer's disease, and the extended triphenylalanine peptide which forms a range of distinct nanostructures *in vitro*. We found that the aggregation propensity, regarding the critical monomer concentration, strongly increases with size, with triphenylalanine being the most aggregation prone species under our experimental conditions. In the context of classical nucleation theory, this increase in aggregation propensity can be attributed to the larger free energy decrease upon aggregation of larger peptides and is not due to the presence/absence of a peptide bond *per se*. Taken together, this work provides insights into the aggregation processes of chemically simple systems and suggests that both backbone-containing peptides and backbone-lacking amino acids assemble through a similar mechanism, thus supporting the classification of amino acids in the continuum of amyloid-forming building blocks.

Keywords: phenylalanine, self-assembly, aggregation, turbidity, thermodynamics, nucleation

Introduction

The formation of supramolecular aggregates is a hallmark of a wide range of human disorders. For instance, peptide and protein aggregation is commonly associated with neurodegenerative conditions, such as Alzheimer's or Parkinson's disease.[1] In inborn error of metabolism (IEM) disorders, such as phenylketonuria (PKU) and hyperoxaluria, it are small metabolites that form ordered assemblies.[2–4] However, the process of aggregation at the molecular level, especially nucleation, is not well understood.[5–7] Specifically, a detailed understanding of the molecular events that lead to nucleation is critical for the prediction of prognosis as well as for the development of innovative therapeutic approaches. This is especially important in the case of IEM disorders as the concentration of the metabolites can be extremely high and thus prone to nucleation and consequent propagation of assembled structures, leading to deleterious effects. Moreover, comparison of the aggregation behaviour of proteins and metabolites will contribute to the comprehensive understanding of the biomolecular aggregation process.

Kinetic and thermodynamic effects govern supramolecular self-organisation.[8] Often, the aggregated state corresponds to the most stable state of these systems, leading to strong thermodynamic driving forces for aggregation.[9] However, there are barriers to aggregation, which can kinetically stabilise the different stages of assemblies as well as the soluble state.[10] This often leads to a nucleated polymerisation mechanism, *i.e.* a process in which an energetically unfavourable process, nucleation, precedes the favourable growth of the aggregated phase. This mechanism is widespread in nature and found, for example, in amyloid formation and molecular crystallisation.[11–13] The size of the nucleus is dependent on the degree of supersaturation of the solution, *i.e.* the ratio of monomer concentration to solubility.

Peptide and protein systems with a wide variety of primary sequences can aggregate.[14,15] Similarly, metabolites with no peptide backbone, such as amino acids, nucleobases and other small biomolecules, can also form amyloid-like ordered structures.[3,4,15,16] A prominent example is the amino acid phenylalanine (Phe) which plays a central role in PKU. Its levels are closely monitored in patients based on the well-established correlation between the blood concentration of Phe and the clinical outcome.[17,18] In patients, the concertation of Phe is in the mM range compared to tens of μM in healthy individuals.[19–21] Furthermore, this amino acid serves as part of a central diphenylalanine (Phe_2) motif of the amyloid beta (Aβ) peptide related to Alzheimer's disease.[22] Both Phe and Phe_2 have been shown to self-assemble into fibrillar structures,[3,22,23] raising the question of whether the peptide backbone plays a fundamental role in the aggregation process as was previously assumed.[24–27]

In the case of phenylalanine structures, we can infer on the process of self-assembly from the crystal packing of the amino acid in its zwitterionic state.[28] The amino acids are organised in a β-sheet-like orientation possessing a typical zig-zag order as observed in β-sheet peptide and protein assemblies. However, unlike the peptide assemblies in which the structures are stabilised by backbone interactions, in the case of the phenylalanine solid-state arrangement, the inter-sheet organisation is stabilised by hydrogen bonding network and π-π stacking interactions to form a supramolecular equivalent of a β-sheet conformation,[16,27] referred to as a "supramolecular β-sheet". [29]

Here, we investigate the role of the peptide backbone in two central aspects of aggregation: thermodynamic stability and nucleation barrier. We used solution concentrations close to supersaturation which resulted in large nucleus sizes. In contrast, for peptides such as Aβ42, *in vitro* aggregation experiments are performed at concentrations orders of magnitude above the supersaturation, and therefore a relatively low constant nucleus size is observed.[30] In both cases, the

concentration range is typically chosen to lead to aggregation within easily accessible experimental time scales. We studied the self-assembly process of three phenylalanine-containing molecules: The single amino acid Phe, the dipeptide Phe_2, and the further extended triphenylalanine (Phe_3) peptide. The backbone-containing peptides and backbone-lacking amino acid tend to assemble through a similar mechanism thus supporting the classification of amino acids in the continuum of amyloid-forming building blocks.[3,4,15,31,32]

Results and Discussion

Energy of peptide bond dominates thermodynamic driving forces

We studied the aggregation of systems consisting purely of Phe building blocks, specifically the amino acid Phe, the dipeptide Phe_2 and the tripeptide Phe_3. To establish the thermodynamic stability of each system with respect to its aggregated state, their solubilities were determined as the soluble monomer concentration in equilibrium with the aggregates formed (see Materials and Methods for details): purified monomeric samples up to concentrations significantly above the solubility were allowed to aggregate at 25 ˚C in PBS, pH 7.4, for 29 h. Aggregates were then removed by ultra-centrifugation and the concentration of monomer remaining in the supernatant was determined by absorbance measurements.[33] As shown in Figure 1a, we found that the solubilities decrease by at least one order of magnitude per additional peptide bond and that this trend follows a power law.[34] For a given peptide or protein, the solubility can vary substantially between different solution conditions, such as solvent, pH and temperature.[35,36] Thus, it is important to note that the phenylalanine-based systems in this study were investigated under identical environmental conditions.

To determine the relative stability of the monomeric state with respect to the aggregated state at a given concentration, the measured solubilities can be converted to chemical potentials. The difference in chemical potential, $\Delta\mu$, between the monomeric and aggregated phase is given by

$$\Delta\mu = \mu_{agg} - \mu_{mon} = RT \ln\left(\frac{c_s}{c}\right) \quad (1)$$

where R is the universal gas constant, T the absolute temperature, c the monomer concentration and c_s the solubility. To compare the different systems, we evaluated $\Delta\mu$ at a constant concentration of amino acids, *i.e.*, at 1 M phenylalanine equivalents, so c_{Phe} = 1 M, c_{Phe_2} = 0.5 M and c_{Phe_3} = 0.33 M where c_{Phe}, c_{Phe_2} and c_{Phe_3} are the total monomer concentrations of Phe, Phe_2 and Phe_3, respectively. We found that the stability of the aggregated phase, relative to the soluble state, increases with the number of peptide bonds (Figure 1b). Interestingly, for both Phe_2 and Phe_3, this increase in energy difference between the soluble and aggregated states is almost the same as the energy required to form the peptide bonds in the respective monomers.[37] Thus, when the absolute stabilities of fibrils are compared, with 1 M of Phe amino acid equivalents as the common reference, the relative stabilities of the fibrils formed from Phe, Phe_2 and Ph_3 are comparble. In other words, in the fibrillar state, the presence of the peptide bond only marginally affects the stability, which is supported by our earlier findings that the molecular structure of fibrils is very similar, regardless of the presence of a peptide bond.[16,29]

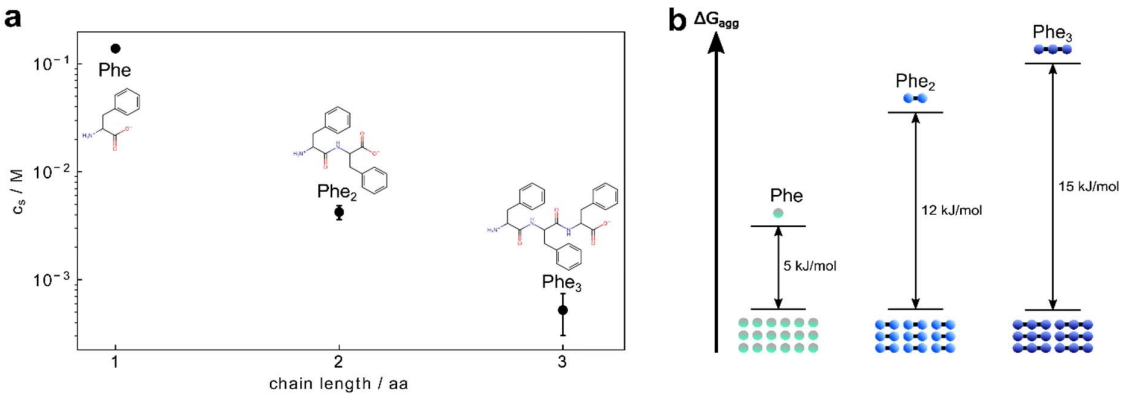

Figure 1: Thermodynamics of peptide self-assembly: (a) The solubility c_s determines the monomer concentration above which the aggregated phase is more stable than the soluble phase. For phenylalanine-derived systems (in PBS pH 7.4, 25 °C) of increasing chain length, the solubility was found to decrease as a power law. (b) The reduced solubility translates into stronger thermodynamic driving forces for aggregation with increasing chain length. The indicated values are with respect to 1 M amino acid equivalent.

Monomer size determines nucleation behaviour

Despite similar thermodynamic driving forces for aggregation, different systems can exhibit distinct kinetic profiles.[38] Provided that the energy barriers between the soluble and the aggregated phase are large enough to control the conversion process, the reaction is under kinetic control. Nucleated polymerisation reactions, such as amyloid formation, are generally kinetically controlled.[38] In such models, the nucleation step requires overcoming the largest energy barrier and thus nucleation acts as an (initial) bottle neck for the formation of a new phase. Once the nucleus has formed, the aggregates grow rapidly by addition of further building blocks from solution. In some cases, existing aggregates can self-replicate, *i.e*. catalyse the formation of new aggregates, for example by fragmentation or secondary nucleation.[38]

Here, we investigated the kinetics of aggregate formation by turbidity assays, a method commonly used to study protein aggregation.[39] This technique is based on the intrinsic light scattering properties of the aggregates. As the aggregation reaction proceeds, the number and size of aggregates increases, leading to a higher scattering intensity. Exemplary time traces of the scattering intensity obtained for Phe are shown in Figure 2a. The traces are sigmoidal in shape, with a flat lag time followed by a sudden increase, which generally indicates the presence of a self-replication mechanism, such as secondary nucleation or fragmentation. Such secondary mechanisms are also observed in the formation of amyloids from larger peptides.[6,38]

A robust and easily determined characteristic of the aggregation kinetics is the lag time, namely the time until a detectable amount of aggregates has formed. In amyloid assembly kinetics, its dependence on the monomer concentration, referred to as the scaling exponent, is used as a guide to determine the aggregation mechanism.[40,41] The lag times, at a range of concentrations for each of the molecules, are shown in Figure 2b, plotted on a double logarithmic plot against the supersaturation, $S = c/c_S$.

One of the most fundamental descriptions of nucleation is provided by classical nucleation theory (CNT), which balances bulk energy gained from forming a new phase with the energy penalty from the interface of two phases, thereby linking the nucleus size to the underlying thermodynamic parameters of the phase change (see SI for details). Using CNT, the dependence of the lag time on the monomer

concentration, through its relation to the nucleus size, can be used to further break nucleation down into its constituent effective driving forces. The main underlying assumptions are local equilibrium conditions, the neglection of finite size effects of the nucleus, and a one-step aggregation mechanism. In this framework, the free energy of a spherical cluster comprising *n* monomers is given by

$$\Delta G(n) = \underbrace{-nk_BT\ln S}_{\text{bulk stabilisation}} + \underbrace{(36\pi v^2)^{1/3}\,\gamma n^{2/3}}_{\text{surface destabilisation}} \quad (2)$$

where k_B is the Boltzmann constant, T the absolute temperature, $S = c/c_S$ the supersaturation, γ the effective surface tension and v the partial volume of a monomer in the condensed phase. The first term on the right-hand side of equation (2) is the integral of equation (1) over the number of monomers in a cluster, *i.e.* describes the relative stabilisation of the aggregated phase. As outlined in the SI, the lag time, τ, can be related to the supersaturation according to

$$\ln\tau = \frac{16\pi v^2\gamma^3}{3{k_B}^3T^3\ln^2 S} + A \quad (3)$$

where A is a constant. The first term on the right-hand side of equation (3) is essentially the nucleation barrier. This term increases as the concentration approaches the solubility and diverges when the concentration equals the solubility. In this limit, the monomeric and aggregated states are equally stable, and the nucleus size approaches infinity. The data of ln(τ) *versus* ln(S) are found to follow our expectations from CNT, and fitting of equation (3), allows us to extract an effective surface tension γ (Table S1) from the slopes of these plots, using the value of v estimated from reported crystal structures.[42–44] We found that there is little variation in the surface tension (per surface area of the clusters) for the different phenylalanine systems tested (Table S1), which is not unexpected given the chemical similarities of the species involved. The implications of this finding on the nucleation kinetics are very interesting. From equation (2), the nucleation barrier and nucleus size can be deduced. Figures 3a and c show plots of these two quantities at a fixed supersaturation. By design, the bulk term only depends on supersaturation and thus is unaffected by the monomer size at constant supersaturation. In contrast, the surface term scales with the monomer size as $v^{2/3}$. Consequently, the increase in molecular volume from the additional amino acid residue(s) increases the surface term along with increasing the number of peptide bonds. Thus, at a given supersaturation, the energy gain by bringing one peptide from solution to the aggregated phase is constant by definition, whereas the energy penalty of the interface depends on the surface area of the interface and thus on the size of the monomer. Therefore, at the same supersaturation, larger peptides show a larger critical nucleus size. By contrast, at the same absolute monomer concentration, the bulk term completely outweighs the surface term (Figure 3b and d). The massive decrease in stability of the monomeric state relative to the aggregated state for the larger peptides described above means that the nucleus size decreases with increasing peptide length. For a small nucleus size, however, the assumption of negligible finite size effects breaks down and CNT ultimately yields an unphysical nucleus size smaller than one monomer. In this limit, there is no barrier for nucleation. In the other limit, when the monomer concentration is below the solubility, aggregation does not occur. This is captured in CNT by an infinitely large nucleus size. Of the systems studied here, Phe solutions were prepared at the lowest supersaturations but highest monomer concentrations. In line with the above, these solutions showed the largest concentration dependence, which indicates the largest nucleus size. This highlights the fact that, when comparing aggregation data, supersaturation rather than absolute monomer concentration should be considered.

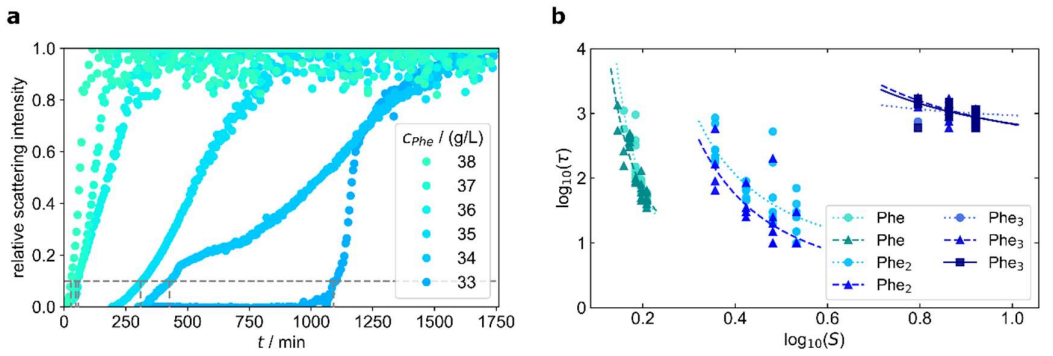

Figure 2: Kinetic barriers for aggregation: (a) Exemplary kinetic traces for Phe. The lag times, τ, were extracted as the times required until the scattering intensity in turbidity assays reached 10% of its plateau value (dashed lines). (b) A double logarithmic plot of the lag time, τ, *versus* supersaturation, S. Dashed lines are best fits to the relationship given through equation (3).

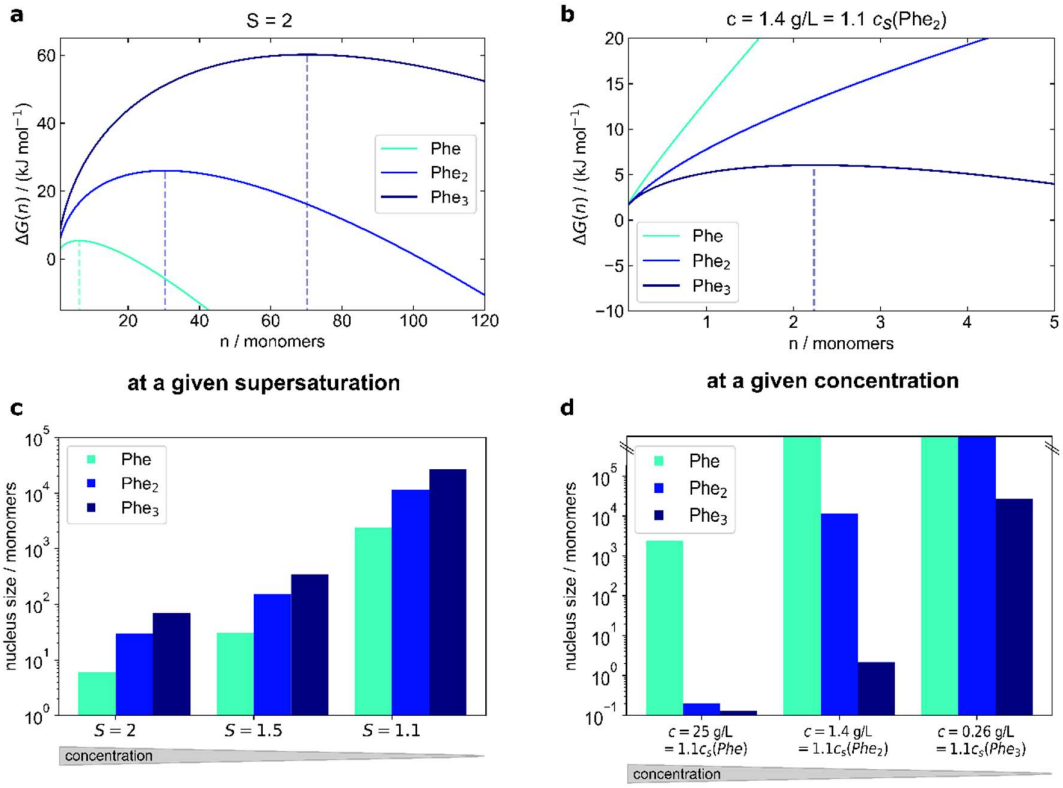

Figure 3: Nucleation barriers and nucleus sizes at constant supersaturation or monomer concentration: Energy profile of nucleation according to equation (2) at (a) a supersaturation of S = 2 and (b) a monomer concentration of 1.4 g/L. Vertical, dashed lines denote the critical point of $\Delta G(n)$. (c) At a given supersaturation, the nucleus size increases for longer chains of (poly-)phenylalanine due to the $v^{2/3}$ dependence of the surface term of equation (2). It also increases with decreasing monomer concentration, as the supersaturation decreases towards one. (d) At a given monomer concentration, however, the nucleus size decreases for longer chains, due to the strong size dependence on the solubility.

In vivo peptide concentrations and implications for disease

As stated above, Phe blood and plasma levels of phenylketonuria patients vary between individuals and are dependent on the compliance to the restrictive diet and the total Phe intake. For most patients with a balanced diet and without severe symptoms, Phe levels are below 360 µM.[20] In the case of patients that do not keep a balanced diet, Phe levels are above 360 µM, neurological symptoms become apparent at 600 µM, and in some patients Phe levels can reach the mM range, up to 1.5 mM.[20,21,45] This is in marked contrast to normal Phe concentration in the range 40-60 µM.[46] As such, the Phe blood and plasma levels even in individuals with phenylketonuria are far below the solubility determined in our *in vitro* experiments ((139 ± 6) mM), *i.e.* in a regime where we would expect no aggregation under *in vitro* conditions. This implies that *in vivo*, local enrichment of Phe or altered thermodynamics due to the biological environment enhance Phe aggregation.

Conclusions

There is a pressing need to understand the forces driving the assembly process of phenylalanine and phenylalanine-containing peptides into well-ordered structures. The aromatic amino acid Phe is prevalent in the sequences of many amyloidogenic peptides and proteins, and accumulates at high concentrations in the IEM disorder PKU.[8,20,47,48] The assembly mechanism of amyloid-like structures by the non-peptide phenylalanine has been challenging to determine. Here, we studied the kinetics and thermodynamics of assembly of Phe into ordered structures in comparison to peptide models as similar as possible to the free amino acid. The use of Phe_2 and Phe_3 allowed us to determine the possible role of a peptide backbone in several aspects of the aggregation process. We find that the stability of the fibril relative to the free amino acid is largely unaffected by the presence of a peptide bond, and that the decreased solubility of larger peptides is mainly a result of the destabilisation of the monomeric state due to the presence of a peptide bond. Given that we found that the effective surface tensions from CNT are comparable for the three species studied here, the kinetic barrier to nucleation at a given supersaturation is higher for larger peptides due to the increased penalty from the effective surface tension, simply as a result of the larger surface area per monomer.

The current work provides a distinct opportunity to understand the aggregation of metabolites associated to pathology. Fluxes of Phe following the consumption and breakdown of proteins result in varied concentrations of Phe in healthy individuals. Intriguingly, the physiological concentrations of Phe are approximately an order of magnitude lower as compared to the critical concertation of 360 µM, in which the symptoms are observed in PKU patients, which are in turn at least two orders of magnitude lower than the solubilities we observe under our *in vitro* conditions. We believe that the range of Phe concentrations for individuals with normal metabolism reflects a safety margin lower than the aggregation limit, as was previously studied for proteins. Extensive studies of the critical concentrations of metabolite compared to the upper limit in normal metabolism should shed light on the interplay between nucleation, assembly, and pathological phenomena.

Materials and Methods

Chemicals

Phenylalanine (Phe) (98%) was purchased from Sigma-Aldrich and used as delivered. Diphenylalanine (Phe_2) (98%) and triphenylalanine (Phe_3) (98%) peptides were purchased from Bachem and used as delivered.

Solubility measurements

Solutions of 10 g/L to 30 g/L Phe in PBS buffer (pH 7.4) were assembled overnight at 25 ˚C. The remaining fraction of soluble monomers was separated by centrifugation (Eppendorf 5417R) at 50k RPM for 1 h at 4 ˚C. The monomer concentration in the supernatant, and as such the solubility, was determined *via* absorbance measurements at 257 nm, for which a calibration curve in the range of 2 g/L to 10 g/L Phe was used. The solubility measurements of Phe_2 and Phe_3 were performed analogously, with initial monomer concentrations of 1 g/L to 4 g/L and 0.25 g/L to 1.5 g/L, respectively, and using calibration curves in the range of 0.1 g/L to 0.5 g/L and 0.01 g/L to 0.16 g/L, respectively (Figure S1, Table S1). As the thermodynamic activity coefficient of amino acids is unlikely to significantly deviate from 1 in the applied concentration regime,[49] we did not correct for it. Otherwise, the activity coefficient would enter the equations as a pre-factor for the concentrations, effectively rescaling the concentrations.

Calculation of free energies

The solubilities can be converted to free energies according to equation (1). In order to compare the relative stability of the fibrils formed from Phe, Phe_2 and Phe_3, 1 M Phe equivalents was chosen as a common reference. Stabilities were analysed using a thermodynamic cycle[50] along with estimates of the energy required for peptide bond formation.[37]

Kinetic turbidity assays

A stock solution of 41 g/L Phe in PBS (pH 7.4) was heated to 90 ˚C for 3 h until fully dissolved. To a 96 well plate with clear underside (Greiner bio-one, 655090) 5µL of 2.6 mM thioflavin T (ThT) was added (to a final concentration of 40 µL). A hot PBS-only solution was added at various amounts such that the hot Phe stock solution could be diluted to final concentrations of 30 g/L to 40 g/L within a final volume of 205 µL. The plate was sealed (TempPlate® sealing film, USA scientific) and rapidly transferred into a CLARIOstar plate reader (BMG). Turbidity absorbance was measured at 405 nm. The measurements were taken in 5 min intervals for 350 cycles at 25 ˚C. Stock solutions of 5 g/L Phe_2 and 2.5 g/L Phe_3 were prepared in the same manner and diluted in hot PBS solution to final concentrations ranging from 0.5 g/L to 4 g/L for Phe_2 and 0.25 g/L to 2 g/L for Phe_3. Both Phe_2 and Phe_3 assembly kinetic measurements were conducted as for Phe.

Analysis of kinetic data

The time traces of the turbidity assays were normalised using the online fitting software Amylofit, as outlined in the respective manual.[40] As the full kinetic curves could not be accurately described by our standard models for aggregate formation, we opted instead for a model-free approach that directly extracts the lag time from the data. The lag times, τ, were determined as the times required until the signal reached 10% of its plateau value.

The effective surface tensions, γ, were estimated from the slope of $\ln(\tau)$ against $1/\ln^2(S)$, where $S = c/c_S$ is the supersaturation, according to CNT

$$\ln \tau = \frac{16\pi v^2 \gamma^3}{3k_B{}^3 T^3 \ln^2 S} + A \quad (3)$$

where v is the partial volume of a monomer in the condensed phase, k_B the Boltzmann constant, T the absolute temperature, and A a constant (see SI for derivation). The values of v were estimated from reported crystal structures.[42–44] Errors were estimated from variations between repeats,

measurement, and fitting uncertainties. They were propagated assuming independent sources of errors.

Supporting information

Derivation of equation (3) describing how the effective surface tension and the critical nucleus size can be derived from kinetic data in the framework of CNT. The solubility measurements and effective surface tension values are represented in Figure S1 and Table S1.

Author contributions

The paper was written through contributions of all the authors. All the authors have given approval to the final version of the paper.

Notes

The authors declare no competing financial interest.

Acknowledgments

The authors thank the Nehemia Levtzion for Excellent Ph.D. Student from Periphery Regions Scholarship (D.Z.), the Bioinnovators Fellowship & Mentorship by Teva (D.Z.), and the Herchel Smith Fund (M.R.Z.) for supporting this research. D.Z. additionally acknowledges funding from the Israel science foundation (ISF), grants numbers 1558/19 and 802/15. We also thank the European Research Council (grant no. 337969 to G.M. and T.P.J.K), the Newman Foundation (T.P.J.K.), the Oppenheimer Early Career Fellowship (A.L.) and the Centre for Misfolding Diseases (M.R.Z. ,G.M., A.L. and T.P.J.K.) for financial support.

References

(1) Chiti, F.; Dobson, C. M. Protein Misfolding, Functional Amyloid, and Human Disease. *Annu. Rev. Biochem.* **2006**, *75* (1), 333–366. https://doi.org/10.1146/annurev.biochem.75.101304.123901.

(2) Gazit, E. Metabolite Amyloids: A New Paradigm for Inborn Error of Metabolism Disorders. *J. Inherit. Metab. Dis.* **2016**, *39* (4), 483–488. https://doi.org/10.1007/s10545-016-9946-9.

(3) Adler-Abramovich, L.; Vaks, L.; Carny, O.; Trudler, D.; Magno, A.; Caflisch, A.; Frenkel, D.; Gazit, E. Phenylalanine Assembly into Toxic Fibrils Suggests Amyloid Etiology in Phenylketonuria. *Nat. Chem. Biol.* **2012**, *8* (8), 701–706. https://doi.org/10.1038/nchembio.1002.

(4) Zaguri, D.; Shaham-Niv, S.; Naaman, E.; Mimouni, M.; Magen, D.; Pollack, S.; Kreiser, T.; Leibu, R.; Rencus-Lazar, S.; Adler-Abramovich, L.; Perlman, I.; Gazit, E.; Zayit-Soudry, S. Induction of Retinopathy by Fibrillar Oxalate Assemblies. *Commun. Chem.* **2020**, *3* (1), 2. https://doi.org/10.1038/s42004-019-0247-8.

(5) Gaspar, R.; Meisl, G.; Buell, A. K.; Young, L.; Kaminski, C. F.; Knowles, T. P. J.; Sparr, E.; Linse, S. Secondary Nucleation of Monomers on Fibril Surface Dominates α -Synuclein Aggregation and Provides Autocatalytic Amyloid Amplification. *Q. Rev. Biophys.* **2017**, *50*, e6. https://doi.org/10.1017/S0033583516000172.

(6) Cohen, S. I. A.; Vendruscolo, M.; Welland, M. E.; Dobson, C. M.; Terentjev, E. M.; Knowles, T. P. J. Nucleated Polymerization with Secondary Pathways. I. Time Evolution of the Principal Moments. *J. Chem. Phys.* **2011**, *135* (6). https://doi.org/10.1063/1.3608916.

(7) Cohen, S. I. A.; Vendruscolo, M.; Dobson, C. M.; Knowles, T. P. J. Nucleated Polymerization with Secondary Pathways. III. Equilibrium Behavior and Oligomer Populations. *J. Chem. Phys.* **2011**, *135* (6). https://doi.org/10.1063/1.3608918.

(8) Anand, B. G.; Dubey, K.; Shekhawat, D. S.; Kar, K. Intrinsic Property of Phenylalanine to Trigger Protein Aggregation and Hemolysis Has a Direct Relevance to Phenylketonuria. *Sci. Rep.* **2017**, *7* (1), 11146. https://doi.org/10.1038/s41598-017-10911-z.

(9) Levin, A.; Mason, T. O.; Adler-Abramovich, L.; Buell, A. K.; Meisl, G.; Galvagnion, C.; Bram, Y.; Stratford, S. A.; Dobson, C. M.; Knowles, T. P. J. J.; Gazit, E. Ostwalds Rule of Stages Governs Structural Transitions and Morphology of Dipeptide Supramolecular Polymers. *Nat. Commun.* **2014**, *5* (1), 5219. https://doi.org/10.1038/ncomms6219.

(10) Michaels, T. C. T.; Liu, L. X.; Curk, S.; Bolhuis, P. G.; Šarić, A.; Knowles, T. P. J. Reaction Rate Theory for Supramolecular Kinetics: Application to Protein Aggregation. *Mol. Phys.* **2018**, *116* (21–22), 3055–3065. https://doi.org/10.1080/00268976.2018.1474280.

(11) Oxtoby, D. W. Homogeneous Nucleation: Theory and Experiment. *J. Phys. Condens. Matter* **1992**, *4* (38), 7627–7650. https://doi.org/10.1088/0953-8984/4/38/001.

(12) Wetzel, R. Kinetics and Thermodynamics of Amyloid Fibril Assembly. *Accounts of Chemical Research*. **2006**, pp 671–679. https://doi.org/10.1021/ar050069h.

(13) Gazit, E. The "Correctly Folded" State of Proteins: Is It a Metastable State? *Angewandte Chemie - International Edition*. **2002**, pp 257–259. https://doi.org/10.1002/1521-3773(20020118)41:2<257::AID-ANIE257>3.0.CO;2-M.

(14) Levin, A.; Hakala, T. A.; Schnaider, L.; Bernardes, G. J. L.; Gazit, E.; Knowles, T. P. J. Biomimetic Peptide Self-Assembly for Functional Materials. *Nature Reviews Chemistry*. Nature Research

November 1, **2020**, pp 615–634. https://doi.org/10.1038/s41570-020-0215-y.

(15) Shaham-Niv, S.; Adler-abramovich, L.; Schnaider, L.; Gazit, E. Extension of the Generic Amyloid Hypothesis to Nonproteinaceous Metabolite Assemblies. *Sci. Adv.* **2015**, *1* (August), 1–7. https://doi.org/10.1126/sciadv.1500137.

(16) Zaguri, D.; Shaham-Niv, S.; Chakraborty, P.; Arnon, Z.; Makam, P.; Bera, S.; Rencus-Lazar, S.; Stoddart, P. R.; Gazit, E.; Reynolds, N. P. Nanomechanical Properties and Phase Behavior of Phenylalanine Amyloid Ribbon Assemblies and Amorphous Self-Healing Hydrogels. *ACS Appl. Mater. Interfaces* **2020**, *12* (19), 21992–22001. https://doi.org/10.1021/acsami.0c01574.

(17) Arn, P. H. Phenylketonuria (PKU). In *Encyclopedia of the Neurological Sciences*, Second Edition; Academic press: London, **2014**; Volume 1, pp 887–889.

(18) Blau, N.; Van Spronsen, F. J.; Levy, H. L. Phenylketonuria. In *The Lancet*; **2010**; Vol. 376, pp 1417–1427. https://doi.org/10.1016/S0140-6736(10)60961-0.

(19) Hanley, W. B. Adult Phenylketonuria. *American Journal of Medicine*. **2004**, pp 590–595. https://doi.org/10.1016/j.amjmed.2004.03.042.

(20) Van Wegberg, A. M. J.; MacDonald, A.; Ahring, K.; Bélanger-Quintana, A.; Blau, N.; Bosch, A. M.; Burlina, A.; Campistol, J.; Feillet, F.; Giżewska, M.; Huijbregts, S. C.; Kearney, S.; Leuzzi, V.; Maillot, F.; Muntau, A. C.; Van Rijn, M.; Trefz, F.; Walter, J. H.; Van Spronsen, F. J. The Complete European Guidelines on Phenylketonuria: Diagnosis and Treatment. *Orphanet Journal of Rare Diseases*. **2017**. https://doi.org/10.1186/s13023-017-0685-2.

(21) Albrecht, J.; Garbade, S. F.; Burgard, P. Neuropsychological Speed Tests and Blood Phenylalanine Levels in Patients with Phenylketonuria: A Meta-Analysis. *Neuroscience and Biobehavioral Reviews*. **2009**, pp 414–421. https://doi.org/10.1016/j.neubiorev.2008.11.001.

(22) Reches, M.; Gazit, E. Self-Assembly of Peptide Nanotubes and Amyloid-like Structures by Charged-Termini-Capped Diphenylalanine Peptide Analogues. *Isr. J. Chem.* **2005**, *45*, 363–371. https://doi.org/10.1560/5MC0-V3DX-KE0B-YF3J.

(23) Adler-Abramovich, L.; Reches, M.; Sedman, V. L.; Allen, S.; Tendler, S. J. B.; Gazit, E. Thermal and Chemical Stability of Diphenylalanine Peptide Nanotubes: Implications for Nanotechnological Applications. *Langmuir* **2006**, *22* (3), 1313–1320. https://doi.org/10.1021/la052409d.

(24) Gordon, D. J.; Meredith, S. C. Probing the Role of Backbone Hydrogen Bonding in β-Amyloid Fibrils with Inhibitor Peptides Containing Ester Bonds at Alternate Positions. *Biochemistry* **2003**, *42* (2), 475–485. https://doi.org/10.1021/bi0259857.

(25) Marchut, A. J.; Hall, C. K. Side-Chain Interactions Determine Amyloid Formation by Model Polyglutamine Peptides in Molecular Dynamics Simulations. *Biophys. J.* **2006**, *90* (12), 4574–4584. https://doi.org/10.1529/biophysj.105.079269.

(26) Nelson, R.; Eisenberg, D. Structural Models of Amyloid-Like Fibrils. *Advances in Protein Chemistry*. Academic Press January 1, **2006**, pp 235–282. https://doi.org/10.1016/S0065-3233(06)73008-X.

(27) Gazit, E. A Possible Role for π-Stacking in the Self-Assembly of Amyloid Fibrils. *FASEB J.* **2002**, *16* (1), 77–83. https://doi.org/10.1096/fj.01-0442hyp.

(28) Mossou, E.; Teixeira, S. C. M.; Mitchell, E. P.; Mason, S. A.; Adler-Abramovich, L.; Gazit, E.; Forsyth, V. T. The Self-Assembling Zwitterionic Form of l-Phenylalanine at Neutral PH. *Acta Crystallogr. Sect. C Struct. Chem.* **2014**, *70* (3), 326–331.

https://doi.org/10.1107/S2053229614002563.

(29) Bera, S.; Mondal, S.; Rencus-Lazar, S.; Gazit, E. Organization of Amino Acids into Layered Supramolecular Secondary Structures. *Acc. Chem. Res.* **2018**, *51* (9), 2187–2197. https://doi.org/10.1021/acs.accounts.8b00131.

(30) Cohen, S. I. A.; Linse, S.; Luheshi, L. M.; Hellstrand, E.; White, D. A.; Rajah, L.; Otzen, D. E.; Vendruscolo, M.; Dobson, C. M.; Knowles, T. P. J. Proliferation of Amyloid-B42 Aggregates Occurs through a Secondary Nucleation Mechanism. *Proc. Natl. Acad. Sci. U. S. A.* **2013**, *110* (24), 9758–9763. https://doi.org/10.1073/pnas.1218402110.

(31) Singh, P.; Pandey, S. K.; Grover, A.; Sharma, R. K.; Wangoo, N. Understanding the Self-Ordering of Amino Acids into Supramolecular Architectures: Co-Assembly-Based Modulation of Phenylalanine Nanofibrils. *Mater. Chem. Front.* **2021**, *5* (4), 1971–1981. https://doi.org/10.1039/d0qm00784f.

(32) Banerjee, P.; Mondal, D.; Ghosh, M.; Mukherjee, D.; Nandi, P. K.; Maiti, T. K.; Sarkar, N. Selective Self-Assembly of 5-Fluorouracil through Nonlinear Solvent Response Modulates Membrane Dynamics. *Langmuir* **2020**, *36* (10), 2707–2719. https://doi.org/10.1021/acs.langmuir.9b03544.

(33) Goscianska, J.; Olejnik, A.; Pietrzak, R. *In Vitro* Release of L-Phenylalanine from Ordered Mesoporous Materials. *Microporous Mesoporous Mater.* **2013**, *177*, 32–36. https://doi.org/10.1016/j.micromeso.2013.04.021.

(34) Baldwin, A. J.; Knowles, T. P. J.; Tartaglia, G. G.; Fitzpatrick, A. W.; Devlin, G. L.; Shammas, S. L.; Waudby, C. A.; Mossuto, M. F.; Meehan, S.; Gras, S. L.; Christodoulou, J.; Anthony-Cahill, S. J.; Barker, P. D.; Vendruscolo, M.; Dobson, C. M. Metastability of Native Proteins and the Phenomenon of Amyloid Formation. *J. Am. Chem. Soc.* **2011**, *133* (36), 14160–14163. https://doi.org/10.1021/ja2017703.

(35) Mason, T. O.; Chirgadze, D. Y.; Levin, A.; Adler-Abramovich, L.; Gazit, E.; Knowles, T. P. J.; Buell, A. K. Expanding the Solvent Chemical Space for Self-Assembly of Dipeptide Nanostructures. *ACS Nano* **2014**, *8* (2), 1243–1253. https://doi.org/10.1021/nn404237f.

(36) Mason, T. O.; Michaels, T. C. T.; Levin, A.; Dobson, C. M.; Gazit, E.; Knowles, T. P. J.; Buell, A. K. Thermodynamics of Polypeptide Supramolecular Assembly in the Short-Chain Limit. *J. Am. Chem. Soc.* **2017**, *139* (45), 16134–16142. https://doi.org/10.1021/jacs.7b00229.

(37) Martin, R. B. Free Energies and Equilibria of Peptide Bond Hydrolysis and Formation. *Biopolymers* **1998**, *45* (5), 351–353. https://doi.org/10.1002/(sici)1097-0282(19980415)45:5<351::aid-bip3>3.0.co;2-k.

(38) Knowles, T. P. J.; Waudby, C. A.; Devlin, G. L.; Cohen, S. I. A.; Aguzzi, A.; Vendruscolo, M.; Terentjev, E. M.; Welland, M. E.; Dobson, C. M. An Analytical Solution to the Kinetics of Breakable Filament Assembly. *Science (80-.).* **2009**, *326* (5959), 1533–1537. https://doi.org/10.1126/science.1178250.

(39) Zhao, R.; So, M.; Maat, H.; Ray, N. J.; Arisaka, F.; Goto, Y.; Carver, J. A.; Hall, D. Measurement of Amyloid Formation by Turbidity Assay—Seeing through the Cloud. *Biophysical Reviews*. **2016**, pp 445–471. https://doi.org/10.1007/s12551-016-0233-7.

(40) Meisl, G.; Kirkegaard, J. B.; Arosio, P.; Michaels, T. C. T.; Vendruscolo, M.; Dobson, C. M.; Linse, S.; Knowles, T. P. J. Molecular Mechanisms of Protein Aggregation from Global Fitting of Kinetic Models. *Nat. Protoc.* **2016**, *11* (2), 252–272. https://doi.org/10.1038/nprot.2016.010.

(41) Meisl, G.; Rajah, L.; Cohen, S. A. I.; Pfammatter, M.; Šarić, A.; Hellstrand, E.; Buell, A. K.; Aguzzi, A.; Linse, S.; Vendruscolo, M.; Dobson, C. M.; Knowles, T. P. J. Scaling Behaviour and Rate-Determining Steps in Filamentous Self-Assembly. *Chem. Sci.* **2017**, *8* (10), 7087–7097. https://doi.org/10.1039/c7sc01965c.

(42) King, M. D.; Blanton, T. N.; Korter, T. M. Revealing the True Crystal Structure of L-Phenylalanine Using Solid-State Density Functional Theory. *Phys. Chem. Chem. Phys.* **2012**, *14* (3), 1113–1116. https://doi.org/10.1039/c1cp22831e.

(43) Azuri, I.; Adler-Abramovich, L.; Gazit, E.; Hod, O.; Kronik, L. Why Are Diphenylalanine-Based Peptide Nanostructures So Rigid? Insights from First Principles Calculations. *J. Am. Chem. Soc.* **2014**, *136* (3), 963–969. https://doi.org/10.1021/ja408713x.

(44) Gilboa, B.; Lafargue, C.; Handelman, A.; Shimon, L. J. W.; Rosenman, G.; Zyss, J.; Ellenbogen, T. Strong Electro-Optic Effect and Spontaneous Domain Formation in Self-Assembled Peptide Structures. *Adv. Sci.* **2017**, *4* (9), 1700052. https://doi.org/10.1002/advs.201700052.

(45) Bartus, A.; Palasti, F.; Juhasz, E.; Kiss, E.; Simonova, E.; Sumanszki, C.; Reismann, P. The Influence of Blood Phenylalanine Levels on Neurocognitive Function in Adult PKU Patients. *Metab. Brain Dis.* **2018**, *33* (5), 1609–1615. https://doi.org/10.1007/s11011-018-0267-6.

(46) Chakraborty, P.; Gazit, E. Amino Acid Based Self-Assembled Nanostructures: Complex Structures from Remarkably Simple Building Blocks. *ChemNanoMat*. **2018**, pp 730–740. https://doi.org/10.1002/cnma.201800147.

(47) Stanković, I. M.; Niu, S.; Hall, M. B.; Zarić, S. D. Role of Aromatic Amino Acids in Amyloid Self-Assembly. *International Journal of Biological Macromolecules*. **2020**, pp 949–959. https://doi.org/10.1016/j.ijbiomac.2020.03.064.

(48) Gazit, E. A Possible Role for Π-stacking in the Self-assembly of Amyloid Fibrils. *FASEB J.* **2002**, *16* (1), 77–83. https://doi.org/10.1096/fj.01-0442hyp.

(49) Shadloo, A.; Peyvandi, K. Thermodynamic Modeling of Amino Acid Solutions: A New Perspective on CPA EOS. *J. Chem. Thermodyn.* **2018**, *124*, 21–31. https://doi.org/10.1016/j.jct.2018.04.016.

(50) Atkins, P.; de Paula, J., Keeler, J. *Atkin's Physical Chemistry*, Eleventh Edition; Oxford University Press: Oxford and New York, **2018**.